Synthesis of superconducting hcp-ZrH_3 under high hydrogen pressure

Mikhail A. Kuzovnikov,[1,*] Vladimir E. Antonov,[2] Valery I. Kulakov,[2] Vitaly D. Muzalevsky,[2] Nikita S. Orlov,[2] Andrey V. Palnichenko,[2] and Yury M. Shulga[3]

[1]*Centre for Science at Extreme Conditions and School of Physics and Astronomy, University of Edinburgh, Edinburgh EH9 3FD, United Kingdom*

[2]*Institute of Solid State Physics RAS, 142432 Chernogolovka, Moscow District, Russia*

[3]*Institute of Problems of Chemical Physics RAS, 142432 Chernogolovka, Moscow District, Russia*

(Received 15 September 2022; accepted 12 January 2023; published 13 February 2023)

Zirconium trihydride and, for comparison, trideuteride with hexagonal close-packed (hcp) metal lattices were synthesized at a hydrogen/deuterium pressure of 9 GPa and a temperature of 873 K using toroid-type high-pressure chambers. After a rapid cooling (quenching) to 100 K and lowering the pressure to atmospheric, the quenched sample was removed from the chamber and studied by hot extraction analysis, powder x-ray diffraction, and ac magnetic susceptometry. The hot extraction showed that thermal decomposition of both hcp-ZrH_3 and hcp-ZrD_3 in vacuum begins after heating at a rate of 10 K/min to ~200 K and almost ceases at 270 K, leaving tetragonal ε-ZrH_2/ε-ZrD_2 as a result. The x-ray diffraction study at 85 K gave lattice parameters $a = 3.443(2)$ Å and $c = 5.964(4)$ Å for hcp-ZrH_3 and somewhat smaller values of $a = 3.430(5)$ Å and $c = 5.947(5)$ Å for hcp-ZrD_3. The measurements of magnetic susceptibility revealed superconductivity with an onset at 11.6(1) K for hcp-ZrH_3 and 9.5(2) K for hcp-ZrD_3.

DOI: 10.1103/PhysRevMaterials.7.024803

I. INTRODUCTION

High hydrogen pressure is an efficient tool for the synthesis of metal hydrides because compression leads to a sharp increase in the Gibbs free energy of molecular hydrogen due to its large molar volume, and this shifts the metal/hydrogen equilibrium toward the formation of hydrides. In recent years, the high-pressure synthesis of new hydrides has been mainly motivated by the desire to discover materials with anomalously high superconducting temperatures T_c enhanced by the interaction of electrons with optical vibrations of hydrogen atoms. The most impressive results have been obtained over the past 3 years in experiments using high-pressure cells with diamond anvils (DACs). These were the discoveries of hexagonal close packed (hcp) CeH_9 with $T_c = 57$ K and face centered cubic (fcc) CeH_{10} with $T_c = 115$ K [1], hcp-ThH_9 with $T_c = 146$ K, fcc-ThH_{10} with $T_c = 159-161$ K [2], body centered cubic (bcc) CaH_6 with $T_c = 215$ K [3], bcc-YH_6 with $T_c = \sim 220$ K [4,5], hcp-YH_9 with $T_c = 243$ K [5], and fcc-LaH_{10} with $T_c = 250-260$ K [6,7]. An overview of binary hydrides recently synthesized in DACs can be found in Ref. [8].

The above superhydrides can rather be considered as atomically ordered solid metal solutions in hydrogen. For many of them, the composition, crystal structure, and superconducting transition temperature were first predicted by *ab initio* calculations. The T_c values were calculated assuming the conventional phonon-mediated Bardeen-Cooper-Schrieffer (BCS) mechanism of superconductivity [9], and some predictions proved to be surprisingly accurate. For example, the calculations [10,11] gave $T_c \approx 280$ K for fcc-LaH_{10} at a hydrogen pressure of 200 GPa, which was in good agreement with the experimental value of $T_c \approx 250$ K at 150 GPa [6,7]. In addition, every deuterium-substituted superhydride studied to date (hcp-CeD_9 [1], bcc-YD_6 [4,5], hcp-YD_9 [5], and fcc-LaD_{10} [6]) has shown a normal isotope effect (lower T_c of the deuteride than the corresponding hydride with a lighter hydrogen isotope), also in line with the BCS theory.

In contrast to the superhydrides, the four superconducting hydrides that were previously known are not conventional superconductors. Three of them (fcc-PdH with $T_c \approx 9$ K [12], face-centered orthorhombic $TiH_{0.71}$ with $T_c = 4.3$ K [13,14], and hcp-$MoH_{1.2}$ with $T_c = 0.92$ K [15]) demonstrated an inverse isotope effect, and one hydride (cubic cI16-Th_4H_{15} with $T_c \approx 8.2$ K [16]) showed no isotope effect, which is also inconsistent with the BCS theory.

Strange as it may seem, after ~50 years of experimental and theoretical studies of superconductivity of palladium hydrides and deuterides, the origin of the inverse isotope effect is still unclear. The problem was discussed in detail in the review paper in Ref. [17]. The widely held opinion that the inverse isotope effect in the Pd-H/D system is due to the interaction of electrons with strongly anharmonic optical vibrations of hydrogen/deuterium atoms [18] turned out to be untenable since the optical spectra of PdH and PdD studied by inelastic neutron scattering (INS) and averaged over all directions in the crystals showed an almost harmonic behavior [19,20]. The optical spectra of $MoH_{1.1}$ and $MoD_{\sim 1.1}$ were also studied by INS and proved to be almost harmonic [21]. The currently available *ab initio* calculations [22] failed to determine the correct sign of the isotope effect for the Mo-H/D system (the calculations gave $T_c = 3.675$ and 3.522 K for molybdenum monohydride and monodeuteride, respectively,

*m.kuzovnikov@ed.ac.uk

compared with experimental values of $T_c = 0.92$ and 1.11 K from Ref. [15]).

Thus, each of the studied superconducting hydrides with a modest hydrogen content, up to the hydrogen-to-metal atomic ratio $x = 3.75$ in Th_4H_{15}, exhibited the inverse isotope effect. Attempts to find an explanation for this phenomenon have so far been unsuccessful, and it was not even known whether the inverse isotope effect is a general property of such hydrides. One of the experimental ways to solve the last problem is the synthesis and study of new superconducting hydrides with $x \leqslant 3.75$.

Using a DAC, we recently synthesized a previously unknown zirconium hydride of the provisional composition Zr_4H_{15} [23], which was later shown to be a superconductor with $T_c = 4.0$ K at 40 GPa [24]. The formation pressure of this hydride at room temperature was 8.2 GPa [23], which gave us a chance to synthesize it in a relatively large amount using our toroid-type hard-alloy high-pressure chambers generating pressures up to 9 GPa. Combined with the available technique of cooling the samples under pressure to liquid N_2 temperature, this would allow us to maintain the hydride sample in a metastable state at atmospheric pressure and low temperature for further studies of its hydrogen content and other properties that cannot yet be investigated in a DAC (in particular, the Meissner effect, which proves the occurrence of superconductivity, has only been demonstrated for bcc-H_3S [25,26] and fcc-LaH_{10} [26]).

In the experiments [24] carried out at hydrogen pressures from 30 to 93 GPa, the Zr_4H_{15} phase was always observed mixed with another new phase, which was identified as bcc-ZrH_3 and proved to be a superconductor with $T_c = 6.4$ K at 40 GPa. However, neither Zr_4H_{15} nor bcc-ZrH_3 were formed in our experiments at a hydrogen pressure of 9 GPa. Instead, at this pressure and temperatures of 500–700 °C, the formation of a hydride hcp-ZrH_3 was observed.

In this paper, we report on the high-pressure synthesis of hcp-ZrH_3 and hcp-ZrD_3 and on the results of studying their hydrogen (deuterium) content, crystal structure, and superconductivity in the metastable state at ambient pressure and low temperatures.

II. EXPERIMENTAL

The starting material was a 0.12-mm-thick cold-rolled foil made of iodide-processed Zr metal with a purity of 99.99%. First, we synthesized ∼500 mg of a body-centered tetragonal (bct) phase ε-ZrH_2 by exposing this foil to a hydrogen atmosphere at 1 GPa and 300 °C for 24 h in lentil-type high-pressure chambers [27], using NH_3BH_3 as an internal hydrogen source. The method of hydrogenation is described elsewhere [28]. The ε-ZrH_2 phase was the highest zirconium hydride known until recently. The ε-ZrH_2 sample synthesized in this paper was thermally stable under ambient conditions and very brittle. Portions of this sample weighing ∼25 mg each were then powdered in an agate mortar and additionally hydrogenated at 9 GPa and different temperatures from 250 to 700 °C in toroid-type high-pressure chambers [27] using the same method [28]. The quantity of NH_3BH_3 placed in the reaction cell was large enough to ensure that the amount of the released H_2 gas always exceeded the amount of hydrogen absorbed by the sample by 2–3 times. The pressure in the reaction cell was estimated with an accuracy of ±0.5 GPa using the pressure/ram load dependence determined in separate experiments. The temperature was measured with an accuracy of ±10 °C using a Chromel-Alumel thermocouple. The hydrogenation time varied from 24 h at 250 °C to 25 min at 600–700 °C. After the hydrogenation was completed, the sample was quickly cooled (quenched) together with the chamber to ∼−170 °C; the pressure was released; the chamber was disassembled under liquid nitrogen; and the sample was removed from the chamber and further stored in liquid nitrogen to prevent hydrogen losses. Zirconium deuterides were synthesized in the same way using AlD_3 as an internal deuterium source. Since the Al particles formed after the thermal decomposition of AlD_3 were chemically active, the sample was isolated from the AlD_3 powder by a layer of chemically inert hexagonal boron nitride [28] (to be on the safe side, the samples were also separated from NH_3BH_3 by a layer of h-BN in the experiments on high-pressure synthesis of zirconium hydrides).

The hydrogenated and deuterated samples thus prepared were examined by x-ray diffraction at $T = -188$ °C = 85 K with a powder Siemens D500 diffractometer using Cu $K\alpha$ radiation selected by a diffracted beam monochromator. The diffractometer was equipped with a home-designed nitrogen cryostat that permitted loading the samples from a liquid N_2 bath without intermediate warming. Prior to the x-ray investigation, each sample was additionally ground in an agate mortar under liquid nitrogen to reduce texture effects. The obtained diffraction patterns were analyzed by the Rietveld profile refinement method using the POWDERCELL2.4 software [29].

X-ray diffraction studies showed that the samples hydrogenated (deuterated) at 9 GPa and temperatures from 500 to 700 °C partially transformed to the hcp-ZrH_3 (hcp-ZrD_3) phase but always contained some unreacted ε-ZrH_2 (ε-ZrD_2) phase, too. The thermal decomposition of these two-phase samples was studied by hot extraction of the hydrogen (deuterium) into a pre-evacuated calibrated volume in the regime of heating the sample from −186 to 50 °C at a rate of 10 °C min^{-1}. The mass of the analyzed probe was 1–2 mg; the accuracy in determining the ΔH/Zr or ΔD/Zr atomic ratio was 5%. More details on the method used can be found in Ref. [30].

An x-ray diffraction investigation of the two-phase (hcp-ZrH_3 + ε-ZrH_2) samples heated to 50 °C showed that they transformed into the ε-ZrH_2 phase, while the hcp-ZrH_3 phase completely disappeared. Within the experimental error, the lattice parameters of the resulting ε-ZrH_2 phase were the same as previously in the quenched two-phase Zr-H samples and in the initial ε-ZrH_2 sample that suggests an invariable hydrogen content H/Zr of the ε phase. We were unable to determine the exact value of this H/Zr ratio by hot hydrogen extraction because of the very low pressure of gaseous hydrogen in equilibrium with dilute solid hydrogen solutions in α-Zr [31]. In a recent paper [23], weighing a massive sample of zirconium before and after its hydrogenation at 120 bar and 450 °C gave H/Zr = 2.03(2) for the obtained ε dihydride. The stoichiometric composition ZrH_2 for single-phase samples of ε dihydride of zirconium obtained in this paper by any method

was confirmed with an accuracy of 5% with the use of a CHNS analyzer Vario Micro cube (Elementar GmbH, Hanau, Germany) by burning 7-mg portions of the samples in a flow of oxygen at 1200 °C. This analysis also showed the absence of nitrogen, which confirmed that the sample did not react with the h-BN layer surrounding it in the high-pressure cell. At the same time, the analysis revealed traces of carbon. Most likely, this carbon was formed from airborne hydrocarbons adsorbed on the surface of ZrH_2 particles, when the samples were weighed in air prior to the CHNS analysis.

Accordingly, the total hydrogen content $x = \mathrm{H/Zr}$ of the quenched Zr-H samples was determined as $x = 2 + \Delta\mathrm{H/Zr}$, where $\Delta\mathrm{H/Zr}$ was the amount of hydrogen desorbed by hot extraction at temperatures up to 50 °C. For similar reasons, the total deuterium content of Zr-D samples was calculated as $x = 2 + \Delta\mathrm{D/Zr}$.

To determine the temperature T_c of the transition to the superconducting state, temperature dependences of the ac magnetic susceptibility $\chi = \chi' - i\chi''$ of the Zr-H and Zr-D samples were measured using a homemade mutual inductance ac susceptometer analogous to that described in Ref. [32]. A powdered sample with a mass of ~10 mg enclosed in a cylindrical Teflon capsule 4 mm in diameter was placed inside 1 of the 2 identical pickup coils positioned coaxially inside a long vertical excitation coil that provided a uniform ac drive magnetic field with an amplitude of $H_{ac} = 3.5$ mOe and frequency $\nu = 1.5$ kHz at the sample position. Sample transfer was performed without intermediate warming from liquid nitrogen to the measuring system preliminarily cooled to 77 K, which excluded thermal decomposition of the sample. The ac voltages induced in the pickup coils were fed to the differential input of a two-channel lock-in amplifier, which separated the in-phase χ' and out-of-phase χ'' components of the ac susceptibility. More details can be found elsewhere [33]. The susceptibility was measured in regimes of heating and cooling at a rate of 1 K/min. The high thermal conductivity of gaseous helium filling the cryostat ensured small temperature gradients in the powder sample, and the obtained $\chi'(T)$ and $\chi''(T)$ dependences showed no temperature hysteresis. The small difference between the temperatures of the sample and temperature sensor was considered by calibrating the susceptometer with the use of the superconducting transition at $T_c = 9.2$ K in niobium powder placed in the measuring Teflon capsule instead of the Zr-H sample.

III. RESULTS AND DISCUSSION

A. X-ray diffraction

Figure 1(a) shows an x-ray powder diffraction pattern of one of the ε-ZrH_2 samples synthesized at a hydrogen pressure of 1 GPa and temperature of 300 °C and used for the synthesis of hcp-ZrH_3 at higher pressure and temperature.

The rather large residual R factors for ε-ZrH_2 indicated in Fig. 1(a) are mainly due to the anisotropic broadening of diffraction peaks, probably caused by inhomogeneous elastic stresses, which arose during the hydrogenation of zirconium at a relatively low temperature of 300 °C. Diffraction patterns of the unreacted ε-ZrH_2 phase in the two-phase (hcp-ZrH_3 + ε-ZrH_2) samples synthesized from ε-ZrH_2 at 9 GPa, as well as

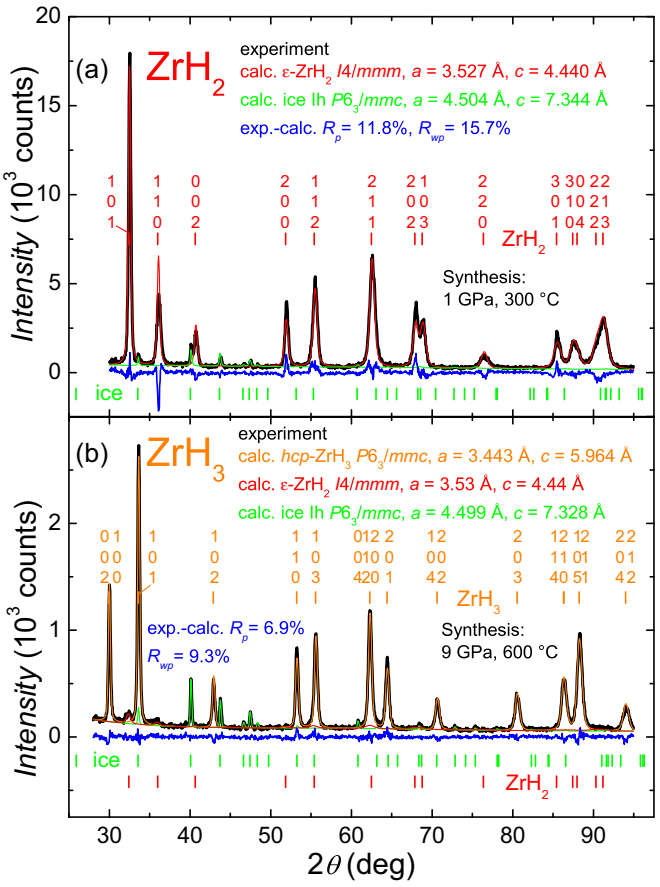

FIG. 1. X-ray powder diffraction patterns and Rietveld refinements of samples of (a) ε-ZrH_2 and (b) hcp-ZrH_3 hydrides synthesized at high hydrogen pressures and studied at ambient pressure and $T = 85$ K using Cu $K\alpha$ radiation. The black curves show the experimental diffraction patterns. The red, orange, and green curves are the calculated contributions from, respectively, ε-ZrH_2, hcp-ZrH_3, and hexagonal ice Ih condensed onto the surface of the sample holder while loading it into the x-ray cryostat. The blue curves are the Rietveld fit residuals.

patterns of the single-phase samples of ε-ZrH_2 resulted from heating those two-phase samples to 50 °C in the course of thermal desorption analysis, looked similar and corresponded to the lattice parameters of the ε-ZrH_2 phase indicated in Fig. 1(a) and Table I. The lattice parameters of the ε-ZrD_2 phase in the studied Zr-D samples did not depend on the sample prehistory either and were somewhat smaller than the parameters of the ε-ZrH_2 phase (see Table I). As discussed in Sec. II, the compositions of ε dihydrides and dideuterides of zirconium formed under high pressures were close to the stoichiometry of ZrH_2 and ZrD_2, respectively.

X-ray diffraction studies showed no changes in the ε-ZrH_2 samples after their additional hydrogenation at 9 GPa and 250 °C. A significant amount of the hcp-ZrH_3 phase always formed at 9 GPa and temperatures from 500 to 700 °C, but the obtained samples still contained some unreacted ε-ZrH_2 phase. The fraction of the hcp-ZrH_3 phase greatly varied from experiment to experiment for samples hydrogenated under the same temperature. For example, the samples synthesized at 9 GPa and 600 °C had the hcp-ZrH_3/ε-ZrH_2 mass ratios from

TABLE I. Composition, crystal structure, synthesis conditions, lattice parameters, and superconducting transition temperature of the Zr-H and Zr-D phases studied in this paper.

Composition, crystal structure	Synthesis conditions	Lattice parameters ($P = 1$ atm, $T = 85$ K)	Superconducting temperature ($P = 1$ atm)
ε-$ZrH_{2.00(5)}$	1 GPa	$a = 3.527(5)$ Å, $c = 4.440(5)$ Å	<2 K
ThH_2-type, *I4/mmm*	300 °C	$c/a = 1.259(6)$	
	24 h	$V = a^2c/2 = 27.62(8)$ Å^3/atom Zr	
ε-$ZrD_{2.00(5)}$	1 GPa	$a = 3.514(5)$ Å, $c = 4.421(5)$ Å	<2 K
ThH_2-type, *I4/mmm*	300 °C	$c/a = 1.259(6)$	
	24 h	$V = a^2c/2 = 27.30(8)$ Å^3/atom Zr	
$ZrH_{3.00(7)}$	9 GPa	$a = 3.443(2)$ Å, $c = 5.964(4)$ Å	11.6(1) K, this paper
hcp, $P6_3/mmc$	600 °C	$c/a = 1.732(2)$	11.7 K [34], calculation
	25 min	$V = \frac{\sqrt{3}}{4}a^2c = 30.61(2)$ Å^3/atom Zr	
$ZrD_{\approx 3}$	9 GPa	$a = 3.430(5)$ Å, $c = 5.947(5)$ Å	9.5(2) K, this paper
hcp, $P6_3/mmc$	600 °C	$c/a = 1.734(6)$	9.21 K [34], calculation
	25 min	$V = \frac{\sqrt{3}}{4}a^2c = 30.30(9)$ Å^3/atom Zr	

48/52 to 94/6. An x-ray diffraction pattern of the sample with a maximum content of 94(3) wt. % of the hcp-ZrH_3 phase is shown in Fig. 1(b). The maximum yield of the hcp-ZrD_3 phase at a D_2 pressure of 9 GPa was also reached at 600 °C, but it was only 37(5) wt. %. The refined parameters of the hcp metal lattice of the ZrH_3 and ZrD_3 phases in these samples are presented in Table I.

The fields of thermodynamic stability of hcp-ZrH_3 and two other high-pressure zirconium hydrides, Zr_4H_{15} [23,24] and bcc-ZrH_3 [24], on the *T-P* phase diagram of the Zr-H system cannot yet be located even approximately. Previous room-temperature experiments showed [23] that Zr_4H_{15} is formed from ε-ZrH_2 at a hydrogen pressure of 8.2 GPa, does not change its composition at pressures up to 39 GPa, and transforms back into ε-ZrH_2 when the pressure is subsequently lowered <3.5 GPa. The reversibility of the reaction suggests the occurrence of phase equilibrium $4ZrH_2 + \frac{7}{2}H_2 = Zr_4H_{15}$ at a certain pressure between 3.5 and 8.2 GPa and the thermodynamic stability of Zr_4H_{15} at pressures above this point.

One more zirconium hydride, bcc-ZrH_3, has been discovered and studied at hydrogen pressures from 30 to 93 GPa [24]. In these experiments, bcc-ZrH_3 coexisted with Zr_4H_{15}, and this two-phase mixture, once formed, did not change its ZrH_3/Zr_4H_{15} ratio with increasing pressure. It cannot be excluded that bcc-ZrH_3 is a metastable intermediate phase without a field of thermodynamic stability on the equilibrium *T-P* diagram.

As shown in this paper, at temperatures from 500 to 700 °C and a pressure of 9 GPa, ε-ZrH_2 transforms into hcp-ZrH_3, and the hydrogenated samples never contain Zr_4H_{15} or bcc-ZrH_3. Therefore, hcp-ZrH_3 is likely to be the most stable hydride at high temperatures and moderate pressures that suggests the occurrence of a triple point ε-ZrH_2+ hcp-ZrH_3 + Zr_4H_{15} on the equilibrium *T-P* diagram. The pressure of the triple point should be <9 GPa and the temperature < 500 °C.

Interestingly, the chemical composition and crystal structure of all three high-pressure hydrides of zirconium obtained experimentally (hcp-ZrH_3, bcc-ZrH_3, and Zr_4H_{15}) were correctly predicted by *ab initio* calculations at $T = 0$ K, whereas the estimates regarding the relative stability of these hydrides were controversial. Some *ab initio* calculations predicted that hcp-ZrH_3 should be stable at hydrogen pressures >0 GPa [34] or 3 GPa [35]. According to these predictions, hydrogen atoms in the $P6_3/mmc$ crystal structure of hcp-ZrH_3 with Zr atoms at $2d$ sites should be ordered at $4f$ tetrahedral interstitial sites and $2b$ planar triangular sites separating octahedral interstices. Some other calculations showed that bcc-ZrH_3 should be stable >0 GPa [36,37], yet one more calculation partially confirmed by experiment [24] suggested that hcp-ZrH_3 is metastable with respect to bcc-ZrH_3, which in its turn is metastable with respect to Zr_4H_{15}, and the latter should be reversibly formed from ε-ZrH_2 at 4 GPa. The pressure of the $4ZrH_2 + \frac{7}{2}H_2 = Zr_4H_{15}$ equilibrium predicted by Xie *et al.* [24] is consistent with experiment [23], while the higher thermodynamic stability of bcc-ZrH_3 compared with hcp-ZrH_3 contradicts experimental results of present paper.

B. Hydrogen desorption

Figure 2 shows the release of gaseous hydrogen (deuterium) into a pre-evacuated volume upon heating the two-phase Zr-H (Zr-D) samples with the maximum content of the hcp-ZrH_3 (hcp-ZrD_3) phases reached in this paper. With a heating rate of 10 °C/min, the gas evolution from both the Zr-H and Zr-D samples begins at ∼−80 °C and almost stops at +20 °C. Heating to a maximum temperature of 50 °C led to the complete decomposition of the hcp-ZrH_3 (hcp-ZrD_3) phases and the formation of single-phase homogeneous ε-ZrH_2 (ε-ZrD_2) samples.

Assuming that the hydrogen content of ε dihydride in the as-quenched Zr-H sample is the same as in the sample after the hot extraction analysis and equals to H/Zr = 2 (see the discussion in Sec. II), the hydrogen content of the hcp trihydride can be estimated as $x = 2 + y/z$, where $y = \Delta$H/Zr is the total amount of hydrogen released from the quenched sample in the process of hot extraction at temperatures up to 50 °C, and z is the mass fraction of the hcp phase in this sample determined by x-ray diffraction. As seen from Fig. 2, $y = 0.87$ for the Zr-H sample with $z = 0.94$, which gives $x = 2 + 0.87(4)/0.94(3) = 2.93(5)$ for the hcp trihydride ZrH_x. Averaging the results for six different Zr-H samples prepared at 9 GPa and 600 °C gives $\langle x \rangle = 2 + (0.87/0.94 + 0.87/0.91 + 0.79/0.80 + 0.73/0.73 +$

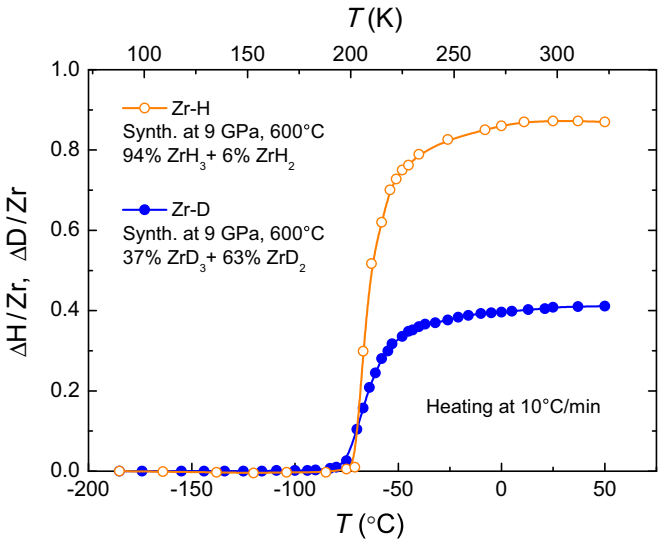

FIG. 2. Temperature dependences of the amount of hydrogen (deuterium) released from quenched two-phase hcp-$ZrH_3 + \varepsilon$-ZrH_2 (hcp-$ZrD_3 + \varepsilon$-ZrD_2) samples heated at 10 °C/min in a closed-volume, pre-evacuated measuring system.

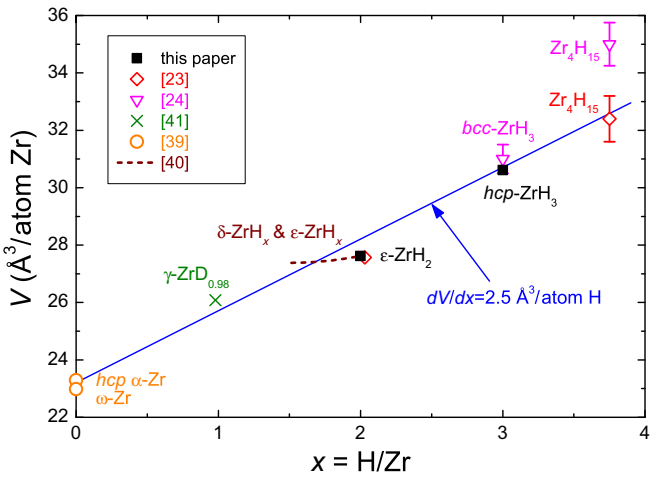

FIG. 3. Atomic volumes V of zirconium hydrides at atmospheric pressure as a function of their hydrogen content $x = \mathrm{H/Zr}$. The point for hcp-ZrH_3 was obtained at $T = 85$ K; the other points refer to room temperature. The points for Zr_4H_{15} [23], Zr_4H_{15}, and bcc-ZrH_3 [24], and the ω phase of Zr metal [39] were determined by extrapolating the experimental dependences $V(P)$ from high pressures to $P = 1$ atm. The segment of the dashed brown curve shows a smooth $V(x)$ dependence for the fcc solid solutions δ-ZrH_x at $1.5 \leqslant x \leqslant 1.7$ and bct solutions ε-ZrH_x at $1.7 \leqslant x \leqslant 1.9$ [40]. The crystal structure of the γ-$ZrD_{0.98(3)}$ phase is orthorhombic, space group *Cccm* [41].

$0.65/0.61 + 0.50/0.48)/6 = 2 + (0.93 + 0.96 + 0.99 + 1.00 + 1.07 + 1.04)/6 = 3.00(7)$, and this value is indicated in Table I (the uncertainty in the $\langle x \rangle$ value thus determined is mainly due to possible systematic instrumental errors).

In a similar way, an estimate of $x = 2 + 0.41(2)/0.37(5) = 3.11(16)$ can be obtained for the hcp trideuteride ZrD_x using the experimental data from Fig. 2. Our studies of other Zr-D samples synthesized at 9 GPa did not improve the accuracy of this estimate because of the much lower yield of the hcp trideuteride. By analogy with hcp-ZrH_3, the trideuteride is likely to be a stoichiometric compound ZrD_3, and this is what we indicated in Table I.

As established in Ref. [23], the value of the atomic volume V of the high-pressure hydride Zr_4H_{15} extrapolated to $P = 1$ atm and plotted as a function of the hydrogen content $x = \mathrm{H/Zr}$ agrees with the approximately linear dependence $V(x)$ for low-pressure zirconium hydrides (Vegard's law for hydrides). As seen from Fig. 3, the experimental $V(x)$ points for hcp-ZrH_3 from this paper and for bcc-ZrH_3 from Ref. [24] also agree with this dependence, whereas the point for Zr_4H_{15} obtained in Ref. [24] lies far apart. We believe that the $V(x)$ value for Zr_4H_{15} at $P = 1$ atm determined in Ref. [23] is more reliable because it was obtained by extrapolating the $V(P)$ dependence measured at pressures down to 3.5 GPa, while the XRD patterns in Ref. [24] were only collected above 30 GPa. In Fig. 3, the straight blue line with the slope $dV/dx = 2.5(1)$ Å^3/atom H is a linear fit to all experimental points shown in the figure, with the exception of Zr_4H_{15} from Ref. [24]. Linear $V(x)$ dependences with a slope of 2–3 Å^3/atom H are typical of hydrides of transition and rare earth metals [38].

C. Magnetic susceptibility

The *ab initio* calculations [34], which predicted the formation of hcp-ZrH_3, also predicted that this hydride should be a superconductor with $T_c = 11.7$ K and that the deuteride hcp-ZrD_3 should have a lower $T_c = 9.21$ K, thus demonstrating the normal isotope effect in accordance with the BCS theory. Results of our measurements of ac magnetic susceptibility presented in Fig. 4 showed that these predictions were remarkably accurate.

After each measurement, the susceptometer was calibrated by the ac susceptibility response to the superconducting transition in a reference sample of niobium powder of the same volume as the studied sample and of a similar shape. This made it possible to use the obtained dependences $\chi'(T)$ and $\chi''(T)$ for a semiquantitative assessment of the effect of shielding the ac magnetic field for the samples under study. As can be seen from the upper panel of Fig. 4(a), the $4\pi\chi'(T)$ dependence for the sample with 94% of the hcp-ZrH_3 phase forms a step characteristic of a superconducting transition at $T_c \approx 11.6$ K and approaches the horizontal line $4\pi\chi' = -1.3$ at lower temperatures. The latter value is not very accurate because it exceeds $4\pi\chi' = -1$ of the ideal diamagnetic. Anyway, such a result signifies a near-perfect shielding of the magnetic field, which can only be observed for a superconductor.

The $4\pi\chi''(T)$ dependence for the sample with 94% ZrH_3 tends to zero at $T \ll 11.6$ K [see the bottom panel of Fig. 4(a)] that indicates a negligibly weak energy dissipation, and this is also a property of the superconducting state. Additionally, the dependence shows an extra-loss peak at 11.6 K, and the occurrence of a similar peak in the temperature range of superconducting transition is characteristic of many materials [42–44]. Thus, the experiment leaves no doubt that the transition observed in hcp-ZrH_3 is a transition to the superconducting state.

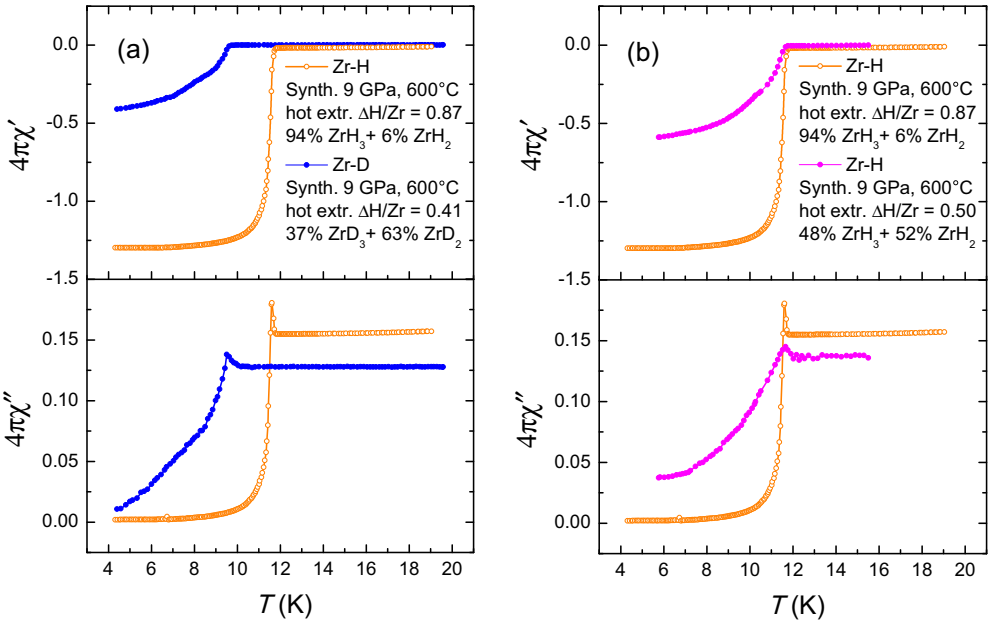

FIG. 4. Temperature dependences of the ac magnetic susceptibility $\chi = \chi' - i\chi''$ in the vicinity of superconducting transition in (a) powdered Zr-H and Zr-D samples containing the hcp-ZrH_3 and hcp-ZrD_3 phases, respectively, and (b) two Zr-H samples with different contents of the hcp-ZrH_3 phase. The real part χ' of the susceptibility is shown in the upper panels, the imaginary part χ'' in the bottom panels. The measurements were carried out in a drive magnetic field with an amplitude of 3.5 mOe and a frequency of 1.5 kHz.

The $4\pi\chi'(T)$ and $4\pi\chi''(T)$ dependences for the Zr-D sample containing 37% of the hcp-ZrD_3 phase are also indicative of a superconducting transition, although the temperature interval of the transition is greatly broadened, and the real and imaginary parts of the magnetic susceptibility do not reach the values for the ideal diamagnetic even at a temperature as low as 4.4 K [see Fig. 4(a)]. The broadening is probably caused by the proximity effect of lowering the superconducting gap near the surface of the fine precipitates of hcp-ZrD_3, which grew through the matrix of nonsuperconducting ε-ZrD_2 during its deuteration under high pressure. Nevertheless, the temperature of the onset of the superconducting transition can be reliably determined from the position of the extra-loss peak in the $4\pi\chi''(T)$ dependence.

In fact, despite the broadened temperature interval of the superconducting transition in the Zr-H sample with 48% ZrH_3, the extra-loss peak in its $4\pi\chi''(T)$ dependence is observed at the same temperature of 11.6 K as in the Zr-H sample with 94% ZrH_3 and a narrow transition interval [see Fig. 4(b)]. Since the reasons lying behind the broadening of the transition in the Zr-H and Zr-D samples are likely to be the same, the peak in the $4\pi\chi''(T)$ dependence for the Zr-D sample with 37% ZrD_3 should apparently be observed at almost the same temperature as in a single-phase ε-ZrD_3 sample.

The values of $T_c = 11.6(1)$ K for the ε-ZrH_3 phase and $T_c = 9.5(2)$ K for the ε-ZrD_3 phase determined from the positions of the extra-loss peaks in the corresponding $4\pi\chi''(T)$ dependences are presented in Table I together with the T_c values predicted by the *ab initio* calculations [34], which assumed a conventional phonon-mediated coupling mechanism of superconductivity. As one can see, the experimental and calculated values almost coincide with each other and demonstrate the normal isotope effect—a lower T_c value for the compound with a heavier hydrogen isotope.

Interestingly, in the Zr-H and Zr-D samples with the low content of ZrH_3 and ZrD_3, respectively, the shielding of the inner parts of the powder particles from the external ac magnetic field by surface supercurrents was incomplete and correlated with the mean content of the superconducting phase. Namely, at the minimum experimental temperature, the real part of the ac magnetic susceptibility reached $4\pi\chi'(4.4\text{ K}) = -0.59$ for the Zr-H sample with 48% ZrH_3 [see Fig. 4(b)] and $4\pi\chi'(5.8\text{ K}) = -0.41$ for the Zr-D sample with 37% ZrD_3 [Fig. 4(a)]. Most likely, complete shielding ($4\pi\chi' = -1$) was not observed because the additional powdering of the samples before their investigation largely destroyed the superconducting shells of trihydride (trideuteride) formed at 9 GPa around the still unreacted dihydride (dideuteride) particles.

Note finally that the hcp-ZrH_3 phase can formally be considered as a solid hydrogen solution in α-Zr with an hcp crystal structure and $T_c \approx 0.6$ K [45]. The absorption of hydrogen up to the composition ZrH_3 then increases the T_c of α-Zr to 11.6 K. Thus far, it is the highest T_c observed in any binary hydride at ambient pressure, apart from the unconfirmed claim of $T_c = 52$–61 K in PdH_x [46]. The hydrogen absorption also leads to a 31% increase in the atomic volume of α-Zr (see Fig. 3), and the volume expansion is anisotropic, as it is accompanied by an increase in the axis ratio of the hexagonal unit cell from $c/a = 1.592(1)$ for α-Zr [39] to $c/a = 1.732(2)$ for hcp-ZrH_3 (Table I).

IV. CONCLUSIONS

Relatively massive samples of a hcp zirconium trihydride synthesized at a hydrogen pressure of 9 GPa and temperatures of 500–700 °C were studied in a metastable state at atmospheric pressure. The superconducting transition in the trihydride was confirmed by the observation of the effect of

shielding the external ac magnetic field, and the trihydride was shown to have the stoichiometric composition ZrH_3. The experimental determination of the hydrogen content of new hydrides is a necessary step in their investigation because hydrides of many transition and rare-earth metals are nonstoichiometric phases with the equilibrium hydrogen concentration that varies greatly depending on the pressure and temperature [38]. For example, hcp dihydride of tantalum, which has been recently found to form at hydrogen pressures of 5.5–41 GPa and room temperature in a DAC [47], had H/Ta = 2.2(1) at 9 GPa and 150 °C [48]. Note in this regard that the hydrogen content of none of the many other hydrides synthesized in the DACs in recent years has ever been studied experimentally, and their compositions have been estimated by comparing the experimental crystal structure of the metal lattice and its atomic volume with the results of *ab initio* calculations performed only for stoichiometric atomic ratios of hydrogen and metal.

The stoichiometric composition ZrH_3 of the hcp zirconium trihydride determined in this paper provided the opportunity to directly compare its experimental and calculated properties, and the superconducting temperature was shown to be perfectly predicted by the calculations [34] including the sign and magnitude of the isotope effect (see Table I). As the superconductivity calculations [34] were based on the BCS theory, the close agreement between the experimental and calculated T_c values for both hcp-ZrH_3 and hcp-ZrD_3 compounds strongly argues in favor of the conventional phonon-mediated coupling mechanism of superconductivity in these phases. Thus, the unusual and yet unexplained inverse isotope effect in all four superconducting hydrides known previously (fcc-PdH, fco-$TiH_{0.71}$, hcp-MoH, and cI16-Th_4H_{15}) is not an inherent property of metal hydrides with moderate values of H/Me $\leqslant$ 3.75. Finding the origin of this effect remains a challenge for theorists and experimenters.

ACKNOWLEDGMENTS

This paper was supported by the Russian Foundation for Basic Research (Grant No. 20-02-00638) and the European Research Council under the European Union's Horizon 2020 research and innovation programme (Grant Agreement No. 948895, MetElOne). Y.M.S. thanks the Ministry of Science and Higher Education of the Russian Federation (State Task No. AAAA-A19-119032690060-9).

[1] W. Chen, D. V. Semenok, X. Huang, H. Shu, X. Li, D. Duan, T. Cui, and A. R. Oganov, High-Temperature Superconducting Phases in Cerium Superhydride with a T_c up to 115 K below a Pressure of 1 Megabar, Phys. Rev. Lett. **127**, 117001 (2021).

[2] D. V. Semenok, A. G. Kvashnin, A. G. Ivanova, V. Svitlyk, V. Yu. Fominski, A. V. Sadakov, O. A. Sobolevskiy, V. M. Pudalov, I. A. Troyan, and A. R. Oganov, Superconductivity at 161 K in thorium hydride ThH_{10}: Synthesis and properties, Mater. Today **33**, 36 (2020).

[3] L. Ma, K. Wang, Y. Xie, X. Yang, Y. Wang, M. Zhou, H. Liu, G. Liu, H. Wang, and Y. Ma, High-Temperature Superconducting Phase in Clathrate Calcium Hydride CaH_6 up to 215 K at a Pressure of 172 GPa, Phys. Rev. Lett. **128**, 167001 (2022).

[4] I. A. Troyan, D. V. Semenok, A. G. Kvashnin, A. V. Sadakov, O. A. Sobolevskiy, V. M. Pudalov, A. G. Ivanova, V. B. Prakapenka, E. Greenberg, A. G. Gavriliuk *et al.*, Anomalous high-temperature superconductivity in YH_6, Adv. Mater. **33**, 2006832 (2021).

[5] P. Kong, V. S. Minkov, M. A. Kuzovnikov, A. P. Drozdov, S. P. Besedin, S. Mozaffari, L. Balicas, F. F. Balakirev, V. B. Prakapenka, S. Chariton *et al.*, Superconductivity up to 243 K in the yttrium-hydrogen system under high pressure, Nat. Commun. **12**, 5075 (2021).

[6] A. P. Drozdov, P. P. Kong, V. S. Minkov, S. P. Besedin, M. A. Kuzovnikov, S. Mozaffari, L. Balicas, F. Balakirev, D. Graf, V. B. Prakapenka *et al.*, Superconductivity at 250 K in lanthanum hydride under high pressures, Nature (London) **569**, 528 (2019).

[7] M. Somayazulu, M. Ahart, A. K. Mishra, Z. M. Geballe, M. Baldini, Y. Meng, V. V. Struzhkin, and R. J. Hemley, Evidence for Superconductivity above 260 K in Lanthanum Superhydride at Megabar Pressures, Phys. Rev. Lett. **122**, 027001 (2019).

[8] M. A. Kuzovnikov, V. S. Minkov, S. Chariton, V. B. Prakapenka, and M. I. Eremets, Synthesis of osmium hydride under high hydrogen pressure, Phys. Rev. B **102**, 214109 (2020).

[9] J. Bardeen, L. N. Cooper, and J. R. Schrieffer, Theory of superconductivity, Phys. Rev. **108**, 1175 (1957).

[10] F. Peng, Y. Sun, C. J. Pickard, R. J. Needs, Q. Wu, and Y. Ma, Hydrogen Clathrate Structures in Rare Earth Hydrides at High Pressures: Possible Route to Room-Temperature Superconductivity, Phys. Rev. Lett. **119**, 107001 (2017).

[11] H. Liu, I. I. Naumov, R. Hoffmann, N. W. Ashcroft, and R. J. Hemley, Potential high-T_c superconducting lanthanum and yttrium hydrides at high pressure, Proc. Nat. Acad. Sci. USA **114**, 6990 (2017).

[12] B. Stritzker and W. Buckel, Superconductivity in the palladium-hydrogen and the palladium-deuterium systems, Z. Phys. **257**, 1 (1972).

[13] I. O. Bashkin, V. E. Antonov, and E. G. Ponyatovsky, Superconductivity of high-pressure phases in the metal-hydrogen systems, in *Studies of High Temperature Superconductors, Vol. 45: Cuprates and Some Unconventional Systems*, edited by A. Narlikar (Nova Science Publishers, New York, 2003), p. 171.

[14] A. I. Kolesnikov, A. M. Balagurov, I. O. Bashkin, V. K. Fedotov, V. Yu. Malyshev, G. M. Mironova, and E. G. Ponyatovsky, A real-time neutron diffraction study of phase transitions in the Ti-D system after high-pressure treatment, J. Phys.: Condens. Matter **5**, 5045 (1993).

[15] V. E. Antonov, I. T. Belash, O. V. Zharikov, A. I. Latynin, and A. V. Palnichenko, Superconductivity of molybdenum hydride and deuteride, Fiz. Tverd. Tela **30**, 598 (1988) [Sov. Phys. Solid State **30**, 344 (1988)].

[16] C. B. Satterthwaite and I. L. Toepke, Superconductivity of Hydrides and Deuterides of Thorium, Phys. Rev. Lett. **25**, 741 (1970).

[17] V. E. Antonov, V. K. Fedotov, A. S. Ivanov, A. I. Kolesnikov, M. A. Kuzovnikov, M. Tkacz, and V. A. Yartys, Lattice dynamics of high-pressure hydrides studied by inelastic neutron scattering, J. Alloys Compd. **905**, 164208 (2022).

[18] I. Errea, M. Calandra, and F. Mauri, First-Principles Theory of Anharmonicity and the Inverse Isotope Effect in Superconducting Palladium-Hydride Compounds, Phys. Rev. Lett. **111**, 177002 (2013).

[19] D. K. Ross, V. E. Antonov, E. L. Bokhenkov, A. I. Kolesnikov, E. G. Ponyatovsky, and J. Tomkinson, Strong anisotropy in the inelastic neutron scattering from PdH at high energy transfer, Phys. Rev. B **58**, 2591 (1998).

[20] V. E. Antonov, A. I. Davydov, V. K. Fedotov, A. S. Ivanov, A. I. Kolesnikov, and M. A. Kuzovnikov, Neutron spectroscopy of H impurities in PdD: Covibrations of the H and D atoms, Phys. Rev. B **80**, 134302 (2009).

[21] M. A. Kuzovnikov, V. E. Antonov, T. Hansen, A. S. Ivanov, A. I. Kolesnikov, V. I. Kulakov, V. D. Muzalevsky, S. Savvin, and M. Tkacz, Isotopic dependence of the frequency of optical vibrations in molybdenum monohydride, J. Alloys Compd. **893**, 162299 (2022).

[22] Z. Liao, C. Liu, Y. Zhang, Y. Guo, and X. Ke, First-principles study on crystal structures and superconductivity of molybdenum hydrides under high pressure, J. Appl. Phys. **128**, 105901 (2020).

[23] M. A. Kuzovnikov and M. Tkacz, High-pressure synthesis of novel polyhydrides of Zr and Hf with a Th_4H_{15}-type structure, J. Phys. Chem. C **123**, 30059 (2019).

[24] H. Xie, W. Zhang, D. Duan, X. Huang, Y. Huang, H. Song, X. Feng, Y. Yao, C. J. Pickard, and T. Cui, Superconducting zirconium polyhydrides at moderate pressures, J. Phys. Chem. Lett. **11**, 646 (2020).

[25] I. Troyan, A. Gavriliuk, R. Rüffer, A. Chumakov, A. Mironovich, I. Lyubutin, D. Perekalin, A. P. Drozdov, and M. I. Eremets, Observation of superconductivity in hydrogen sulfide from nuclear resonant scattering, Science **351**, 1303 (2016).

[26] V. S. Minkov, S. L. Bud'ko, F. F. Balakirev, V. B. Prakapenka, S. Chariton, R. J. Husband, H. P. Liermann, and M. I. Eremets, Magnetic field screening in hydrogen-rich high-temperature superconductors, Nat. Commun. **13**, 3194 (2022).

[27] L. G. Khvostantsev, V. N. Slesarev, and V. V. Brazhkin, Toroid type high-pressure device: History and prospects, High Pressure Res. **24**, 371 (2004).

[28] V. E. Antonov, B. M. Bulychev, V. K. Fedotov, D. I. Kapustin, V. I. Kulakov, and I. A. Sholin, NH_3BH_3 as an internal hydrogen source for high pressure experiments, Int. J. Hydrogen Energy **42**, 22454 (2017).

[29] W. Kraus and G. J. Nolze, POWDER CELL—A program for the representation and manipulation of crystal structures and calculation of the resulting x-ray powder patterns, J. Appl. Cryst. **29**, 301 (1996).

[30] I. O. Bashkin, V. E. Antonov, A. V. Bazhenov, I. K. Bdikin, D. N. Borisenko, E. P. Krinichnaya, A. P. Moravsky, A. I. Harkunov, Y. M. Shul'ga, Y. A. Ossipyan *et al.*, Thermally stable hydrogen compounds obtained under high pressure on the basis of carbon nanotubes and nanofibers, JETP Lett. **79**, 226 (2004).

[31] F. Ricca and T. A. Giorgi, Equilibrium pressures of hydrogen dissolved in a-zirconium, J. Phys. Chem. **71**, 3627 (1967).

[32] D.-X. Chen and V. Skumryev, Calibration of low-temperature ac susceptometers with a copper cylinder standard, Rev. Sci. Instrum. **81**, 025104 (2010).

[33] N. S. Sidorov, A. V. Palnichenko, D. V. Shakhrai, V. V. Avdonin, O. M. Vyaselev, and S. S. Khasanov, Superconductivity of Mg/MgO interface formed by shock-wave pressure, Physica C **488**, 18 (2013).

[34] Z.-Z. Han, Y. Lu, W. Wang, Z.-L. Hou, and X.-H. Shao, The novel structure and superconductivity of zirconium hydride, Comput. Mater. Sci. **134**, 38 (2017).

[35] N. Bourgeois, J.-C. Crivello, P. Cenedese, and J.-M. Joubert, Systematic first-principles study of binary metal hydrides, ACS Comb. Sci. **19**, 513 (2017).

[36] X.-F. Li, Z.-Y. Hu, and B. Huang, Phase diagram and superconductivity of compressed zirconium hydrides, Phys. Chem. Chem. Phys. **19**, 3538 (2017).

[37] K. Abe, High-pressure properties of dense metallic zirconium hydrides studied by *ab initio* calculations, Phys. Rev. B **98**, 134103 (2018).

[38] Y. Fukai, *The Metal-Hydrogen System*, 2nd ed. (Springer-Verlag, Berlin, Heidelberg, 2005), p. 104.

[39] Y. Zhao, J. Zhang, C. Pantea, J. Qian, L. L. Daemen, P. A. Rigg, R. S. Hixson, G. T. Gray, III, Y. Yang, L. Wang *et al.*, Thermal equations of state of the α, β, and ω phases of zirconium, Phys. Rev. B **71**, 184119 (2005).

[40] R. C. Bowman, Jr., B. D. Craft, J. S. Cantrell, and E. L. Venturini, Effects of thermal treatments on the lattice properties and electronic structure of ZrH_x, Phys. Rev. B **31**, 5604 (1985).

[41] A. I. Kolesnikov, A. M. Balagurov, I. O. Bashkin, A. V. Belushkin, E. G. Ponyatovsky, and M. Prager, Neutron scattering studies of ordered gamma-ZrD, J. Phys.: Condens. Matter **6**, 8977 (1994).

[42] T. Nakajima, M. Isino, and E. Kanda, Nonlinear pressure dependence of the superconducting transition temperature of copper sulfide CuS, J. Phys. Soc. Jpn. **28**, 369 (1970).

[43] R. A. Hein, H. Hojaji, A. Barkatt, H. Shafii, K. A. Michael, A. N. Thorpe, M. F. Ware, and S. Alterescu, The low magnetic field properties of superconducting bulk yttrium barium copper oxide-sintered versus partially melted material, J. Supercond. **2**, 427 (1989).

[44] R. B. Goldfarb, M. Lelental, and C. A. Thompson, *Alternating-Field Susceptometry and Magnetic Susceptibility of Superconductors* (Plenum Press, New York, 1991).

[45] B. W. Roberts, Survey of superconductive materials and critical evaluation of selected properties, J. Phys. Chem. Ref. Data **5**, 581 (1976).

[46] H. M. Syed, T. J. Gould, C. J. Webb, and E. MacA. Gray, Superconductivity in palladium hydride and deuteride at 52–61 kelvin, arXiv:1608.01774.

[47] M. A. Kuzovnikov, M. Tkacz, H. Meng, D. I. Kapustin, and V. I. Kulakov, High-pressure synthesis of tantalum dihydride, Phys. Rev. B **96**, 134120 (2017).

[48] M. A. Kuzovnikov, V. E. Antonov, A. S. Ivanov, T. Hansen, S. Savvin, V. I. Kulakov, M. Tkacz, A. I. Kolesnikov, and V. M. Gurev, Neutron scattering study of tantalum dihydride, Phys. Rev. B **102**, 024113 (2020).